

Dynamic properties of asymmetric double Josephson junction stack with quasiparticle imbalance

S. V. Bakurskiy,^{1,2,3} A. A. Neilo,⁴ N. V. Klenov,^{4,1,2,3,5} I. I. Soloviev,^{1,2,3} and M. Yu. Kupriyanov^{1,2}

¹Skobel'syn Institute of Nuclear Physics, Lomonosov Moscow State University 1(2), Leninskie gory, Moscow 119234, Russian Federation

²Moscow Institute of Physics and Technology, Dolgoprudny, Moscow Region, 141700, Russian Federation

³MIREA - Russian Technological University, 119454 Moscow, Russian Federation

⁴Faculty of Physics, Lomonosov Moscow State University, 119992 Leninskie Gory, Moscow, Russian Federation

⁵All-Russian Research Institute of Automatics n.a. N.L. Dukhov (VNIIA), 127055, Moscow, Russian Federation

(Dated: March 7, 2019)

We study analytically and numerically the influence of the quasiparticle charge imbalance on the dynamics of the asymmetric Josephson stack formed by two inequivalent junctions: the fast capacitive junction JJ_1 and slow non-capacitive junction JJ_2 . We find, that the switching of the fast junction into resistive state leads to significant increase of the effective critical current of the slow junction. At the same time, the initial switching of the slow junction may either increase or decrease the effective critical current of the fast junction, depending on ratio of their resistances and the value of the capacitance. Finally, we have found that the slow quasiparticle relaxation (in comparison with Josephson times) leads to appearance of the additional hysteresis on current-voltage characteristics.

PACS numbers: 74.45.+c, 74.50.+r, 74.78.Fk, 85.25.Cp

I. INTRODUCTION

Josephson junctions with multilayer structures in a weak link region between superconducting (S) electrodes are of considerable interest for rapidly developing superconducting spintronics¹⁻⁴. The important class of these devices contains thin superconducting layers s inside this area. These spacers additionally support superconducting correlations inside the weak link and permits to increase a critical current of the junctions compare to that with normal spacers^{5,6}. For instance, SFsFS spin valves⁷⁻¹⁰ has in a weak link F_sF three-layer or periodic F_sF structure formed by different ferromagnets (F). The critical current of such devices depends on the mutual orientation of adjacent F layers magnetization vectors. The next class of devices is based on the SISFS structures¹¹⁻¹³. Their weak place contains an insulator (I) and only one F layer. The SISFS spin valves can combine the properties of a fast and energy-efficient element of logic circuits SIs with the possibility of long-term information storage in the form of the direction of the magnetization vector of the F-layer^{14,15} or in the unconventional phase states of the middle s -layer¹⁶⁻¹⁸. The other types of layers also can be considered. The ferromagnetic insulators (FI)^{19,20} or multilayers insulator-ferromagnetic metal F-I²¹ can be used to obtain magnetic properties without strong suppression in s -layer due to inverse proximity effect. Implementation of topological insulators (TI)²² may add into the system 4π periodic component of the current-phase relation.

The practical applications of such devices meet a number of difficulties associated with the lack of understanding of the dynamic processes occurring in them. The accurate consideration of this problem requires the solution of the nonequilibrium equations of the microscopic theory of superconductivity²³. It is a very difficult task even in symmetric structures that do not contain a superconductor in the weak link region²⁴.

In this paper, we analyze the dynamic processes within a simpler phenomenological approach. In it, there are two lumped Josephson junctions connecting in series via thin in-

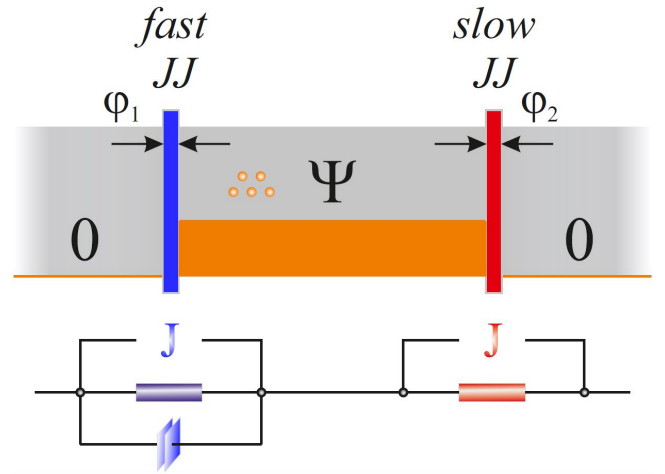


Figure 1: Sketch of the asymmetric double junction stack with equivalent scheme of the circuit in the frame of RSJ-model.

termediate s layer. This s layer is spatially homogeneous and its thickness, d_s , is of order of coherence length, ξ_s , and much smaller than the London penetration depth, λ . The critical currents, $I_{C1,2}$, normal resistances, $R_{1,2}$, and capacitances, $C_{1,2}$, of the junctions are different and junction's dynamics is described by modified resistive shunt model (MRSJ) taking into account coupling processes between the junctions.

In carrying out the necessary modifications of the RSJ model, we used extensive material obtained earlier in the analysis of processes in the stacks of identical tunnel Josephson junctions and multilayer high-temperature superconducting materials²⁵⁻⁴⁶. In these studies, three mechanisms of coupling between Josephson contacts in the stack were identified. They are inductive interaction between adjacent junctions²⁵⁻³², a charge accumulation of condensate³³⁻³⁸ and a quasiparticle accumulation³⁹⁻⁴⁶.

The first two are not relevant for our study. The inductive interaction is important if $d_s > \lambda$ and the width of the stack

is larger than Josephson penetration depth $W > \lambda_J$, while the charge accumulation of condensate occurs when the intermediate s-layer is thinner than the Debye charge screening length λ_D . These conditions are not met in our model.

The quasiparticle accumulation in the intermediate s layer may occur if at least one of the junction in stack is in a resistive state. Under this condition the full current sets in the s film should contain both normal and superconducting components. If the thickness d_s of the s layer is substantially less than the length of the energy relaxation of the quasiparticles injected into it, then a charge imbalance arises in the s film due to the different population of the electron and hole branches of the energy spectrum. The total charge quasi-neutrality is achieved at the same time due to superconducting electrons. It leads to the difference of the gradient-invariant potential of the condensate $\Phi = \Psi$ in the s film from its value in the bulk S electrodes, which is supposed to be in equilibrium, that is having electropotential $\Phi = 0$.

II. MODEL

Following Ryndyk^{39,41} we may write the system of equations of MRSJ model in the form

$$\frac{\partial \varphi_1}{\partial t} = V_1 + \Psi, \quad (1)$$

$$i = \sin \varphi_1 + V_1 + \beta \frac{\partial V_1}{\partial t}, \quad (2)$$

$$\frac{\partial \varphi_2}{\partial t} = V_2 - \Psi, \quad (3)$$

$$i = a \sin \varphi_2 + r V_2, \quad (4)$$

$$\tau_Q \frac{\partial \Psi_1}{\partial t} = -\Psi + \tilde{\kappa} (I_1^{qp} - I_2^{qp}) = -\Psi + \kappa (V_1 - r V_2), \quad (5)$$

$$\kappa = \frac{\tau_Q}{2e^2 R_1 N_0 d_s}. \quad (6)$$

Here times t and τ_Q , currents i , I_1^{qp} , I_2^{qp} , voltages V_1 , V_2 and potential Ψ are normalised on ω_{c1}^{-1} , critical current I_{C1} , and characteristic voltage, $I_{C1} R_1$, respectively, τ_Q is time of quasiparticle relaxation, κ is coupling parameter, e - electron charge, N_0 - density of states of the s film, I_1^{qp} and I_2^{qp} are quasiparticle currents across the junctions. We also introduce the notations $\beta = C_1 2\pi I_{C1} R_1^2 / \Phi_0$, $r = R_1 / R_2$, $a = I_{C2} / I_{C1}$ and assume that capacitance of the second junction is negligibly small and can be omitted. Below we additionally restrict ourself by considering the most interesting for us case in which i is independent in time bias current and there is a large difference between junction's normal resistances, $r \gg 1$, while their critical currents have the same order of magnitude. Then the characteristic frequency of the first junction $\omega_{c1} = 2\pi I_{C1} R_1 / \Phi_0$ is much larger than that of the second one. In this sense we call the first junction as "fast" (implying as it is regular tunnel SIS junction), and call the second junction as "slow" (it can be more complicated structure). The figure 1 shows a schematic representation of the structure under study.

III. FAST QUASIPARTICLE RELAXATION, $\tau_Q \ll 1$

In the limit of fast quasiparticle relaxation in the intermediate s layer in comparison with the characteristic Josephson times $\tau_Q \ll 1$ we can neglect the left side in the kinetic equation (5) and rewrite (1), (3) in the form

$$\frac{\partial \varphi_1}{\partial t} = V_1 + \kappa (V_1 - r V_2), \quad (7)$$

$$\frac{\partial \varphi_2}{\partial t} = V_2 - \kappa (V_1 - r V_2). \quad (8)$$

Equations (7), (8) mean that the interaction between the fast and slow junction is reduced to the redistribution of the electric potential difference between them

$$V_1 = q \frac{\partial \varphi_1}{\partial t} + r p \frac{\partial \varphi_2}{\partial t}, \quad (9)$$

$$V_2 = m \frac{\partial \varphi_2}{\partial t} + p \frac{\partial \varphi_1}{\partial t}, \quad (10)$$

where

$$p = \frac{\kappa}{1 + \kappa + \kappa r}, \quad q = \frac{1 + \kappa r}{1 + \kappa + \kappa r}, \quad m = \frac{1 + \kappa}{1 + \kappa + \kappa r}. \quad (11)$$

Making use of (7), (8) we can rewrite (2), (4) in the closed form for φ_1 and φ_2 forms

$$i = \sin \varphi_1 + q \frac{\partial \varphi_1}{\partial t} + r p \frac{\partial \varphi_2}{\partial t} + \beta q \frac{\partial^2 \varphi_1}{\partial t^2} + \beta r p \frac{\partial^2 \varphi_2}{\partial t^2}, \quad (12)$$

$$i = a \sin \varphi_2 + m r \frac{\partial \varphi_2}{\partial t} + p r \frac{\partial \varphi_1}{\partial t}. \quad (13)$$

A. Slow junction in the superconducting state, $a > 1$

Consider the situation when the fast junction is in the resistive state, while the slow one is in the superconducting state and suppose additionally that $\beta \gg 1$.

Under these conditions we may find solution of equations (12), (13) in the form

$$\varphi_1 = \Omega_1 t + \tilde{\varphi}_1; \quad \varphi_2 = \varphi_{20} + \tilde{\varphi}_2, \quad (14)$$

where $\tilde{\varphi}_1, \tilde{\varphi}_2 \propto \beta^{-1} \ll 1$ - are small periodic in time functions, while Ω_1 and φ_{20} are independent on time frequency of Josephson oscillations of the fast junction and phase difference across the slow junction. Substitution of the (14) into (12) leads to

$$i = \sin \Omega_1 t + \tilde{\varphi}_1 \cos \Omega_1 t + q \Omega_1 + q \frac{\partial \tilde{\varphi}_1}{\partial t} + r p \frac{\partial \tilde{\varphi}_2}{\partial t} + \beta q \frac{\partial^2 \tilde{\varphi}_1}{\partial t^2} + \beta r p \frac{\partial^2 \tilde{\varphi}_2}{\partial t^2}. \quad (15)$$

After averaging over the period oscillation in equation (15), we arrive at

$$i = \langle \tilde{\varphi}_1 \cos \Omega_1 t \rangle + q\Omega_1 \quad (16)$$

and in the zero approximation on β^{-1} for Ω_1 we get.

$$\Omega_1 \simeq iq^{-1}. \quad (17)$$

Taking (17) into account, in the next approximation from (15) we have

$$\frac{\partial^2(q\tilde{\varphi}_1 + pr\tilde{\varphi}_2)}{\partial t^2} = -\frac{\sin \Omega_1 t}{\beta} \quad (18)$$

resulting in

$$q\tilde{\varphi}_1 + pr\tilde{\varphi}_2 = \frac{\sin \Omega_1 t}{\beta\Omega_1^2}, \quad (19)$$

$$q\frac{\partial \tilde{\varphi}_1}{\partial t} + pr\frac{\partial \tilde{\varphi}_2}{\partial t} = \frac{\cos \Omega_1 t}{\beta\Omega_1}, \quad (20)$$

Substitution of (19), (20) into the equation (13) leads to

$$i = a \sin(\varphi_{20} + \tilde{\varphi}_2) + rm\frac{\partial \tilde{\varphi}_2}{\partial t} + \frac{rp}{q}i + \frac{rp \cos \Omega_1 t}{q \beta\Omega_1} - \frac{r^2 p^2}{q} \frac{\partial \tilde{\varphi}_2}{\partial t}, \quad (21)$$

which transforms after some algebra into

$$\frac{i}{(1 + \kappa r)} = \frac{rp \cos \Omega_1 t}{q \beta\Omega_1} + a \sin(\varphi_{20}) + a\tilde{\varphi}_2 \cos(\varphi_{20}) + \frac{r}{(1 + \kappa r)} \frac{\partial \tilde{\varphi}_2}{\partial t}. \quad (22)$$

Averaging over the period oscillation in equation (22) gives the magnitude of effective critical current i_{c2}^* of the slow junction

$$i = i_{c2}^* \sin(\varphi_{20}), \quad i_{c2}^* = a(1 + \kappa r), \quad (23)$$

which exceeds the intrinsic value of the critical current state a .

Taking into account (23) from (22) we further get

$$-pr\frac{\cos \Omega_1 t}{\beta i} = a \cos(\varphi_{20}) \tilde{\varphi}_2 + \frac{r}{(1 + \kappa r)} \frac{\partial \tilde{\varphi}_2}{\partial t}, \quad (24)$$

where for the bias current i set in the positive direction ($i > 0$)

$$\cos(\varphi_{20}) = \frac{\sqrt{a^2(1 + \kappa r)^2 - i^2}}{a(1 + \kappa r)}. \quad (25)$$

The solution of (24) is

$$\tilde{\varphi}_2(t) = -\frac{\kappa r}{\beta\Omega_1} \cos(\Omega_1 t - \varphi_{20}), \quad (26)$$

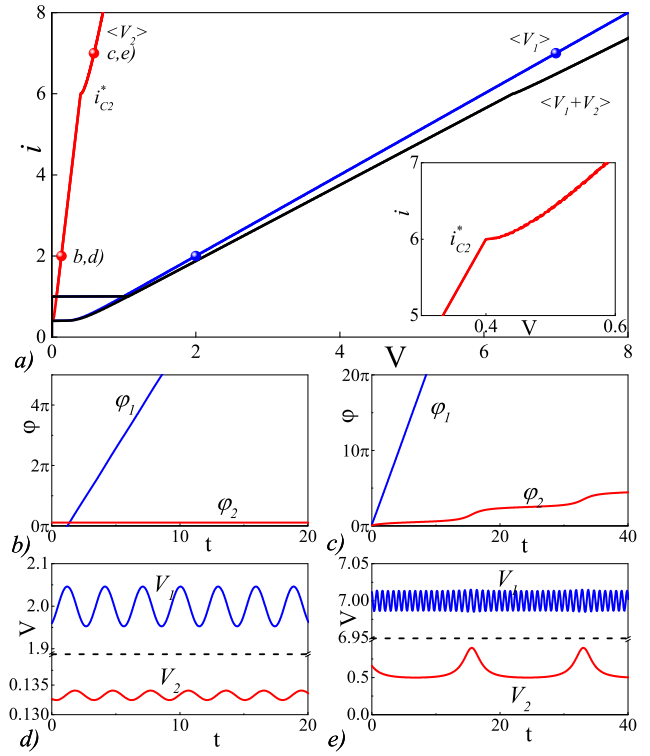


Figure 2: I-V characteristic of the asymmetric Josephson stack with coupling $\kappa = 0.2$. The black line demonstrates the IV dependence of the whole system, the blue line corresponds fast junction and red line describes slow junction. The panels b-e) show phase and voltage dynamics calculated b,c) at the current $i = 2$ below the switch of the slow junction into resistive state and d, e) at the current $i = 7$ over that switch. The other parameters are $r = 10$, $\beta = 10$, and $a = 2$.

leading to

$$\tilde{\varphi}_1(t) = \frac{\sin \Omega_1 t}{q\beta\Omega_1^2} + \frac{\kappa pr^2}{\beta i} \cos(\Omega_1 t - \varphi_{20}). \quad (27)$$

Substitution of (27) into (16) gives the correction to frequency of oscillations Ω_1 in the next approximation in β^{-1}

$$\Omega_1 = \frac{i}{q} - \frac{\kappa pr^2}{2q\beta i} \cos(\varphi_{20}). \quad (28)$$

As a result, the bias current on the fast junction can be represented as the sum of independent on time normal, ($q\Omega_1$), and superconducting parts

$$i = q\Omega_1 + \frac{\kappa pr^2}{2q\beta i} \cos(\varphi_{20}). \quad (29)$$

The normal current components of the bias current is not fully converted into the superconducting one inside the s film, so that there is an accumulation of quasiparticles inside the film. As a consequence, a voltage drop

$$V_2 = m \left(\Omega_1 + \frac{\cos \Omega_1 t}{q\beta\Omega_1} - \frac{\kappa pr^2}{q\beta} \sin(\Omega_1 t - \varphi_{20}) \right) + p \frac{\kappa r}{\beta} \sin(\Omega_1 t - \varphi_{20}) \quad (30)$$

occurs on a slow junction, despite the fact that the total current i is less than its critical one. It means that the slow junction is biased by the superposition of the superconducting and normal current components. As soon as the normal current does not affect the critical one, while the sum of these independent on time components must be equal to external bias i , the critical state of the slow junction must be achieved at larger magnitude of $i = i_{C2}^*$. The critical current enhancement, $i_{C2}^* - a = a\kappa r$ is exactly equal to independent in time normal component of bias current across the slow junction.

To generalize these properties for the case of finite β , we numerically solved Eqs.(7)-(8) for $\beta = 10$. The calculations have been done for coupling parameter $\kappa = 0.2$, the ratio of resistances $r = 10$, and critical current ratio $a = 2$. The Fig. 2a shows current - voltage characteristics (IVC) of the considered structure, where black line respects to whole structure, while blue and red lines correspond to fast $\langle V_1 \rangle$ and slow $\langle V_2 \rangle$ junctions respectively. The points on the curves mark the positions on the IVC at $i = 2$ and $i = 7$ for which the time dependences of the voltages $V_{1,2}$ and phase differences $\varphi_{1,2}$ across the contacts are shown in the Fig. 2b-Fig. 2e.

At the point marked by the letter *b* the slow junction is in the superconducting state. As it is seen in Fig. 2b phase difference φ_2 undergoes oscillations with the frequency Ω_1 around constant over time value, while φ_1 grows linearly with time. The voltage drops $V_{1,2}$ are also oscillated with the frequency Ω_1 relatively the appropriate constant over time values, as it is seen from Fig.2d. At $i = 7$ both junctions are in resistive state. Figures 2c,e give the time evolutions of $\varphi_{1,2}$ and $V_{1,2}$ at $i = 7$ respectively.

The numerical results confirm the analytical estimates. In the full accordance with (9)-(10) when the bias current i exceeds the unity (the critical current of fast junction), there is voltage drop across the structure and it is redistributed between fast and slow junctions. It is also seen that the slow junction starts to generate at $i = i_{C2}^* = a(1 + \kappa r) = 6$. Below this point, the voltage of the slow junction has oscillating component with a frequency of the fast junction, while over the critical current i_{C2}^* it has much smaller frequency.

B. Fast junction in the superconducting state, $a < 1$

In this case, application of the bias current to the structure leads to the switching of the slow junction into the resistive state. At the same time, the fast junction is in a superconducting state despite the fact that in accordance with (9) it has a voltage drop overlaid by the flow of a normal current component across it. In the limit $\beta\Omega_2 \gg 1$, where, Ω_2 , is the frequency of Josephson oscillations of the slow junction. From (12) it follows that as the first approximation on $(\beta\Omega_2)^{-1}$ we can assume that

$$q \frac{\partial^2 \varphi_1}{\partial t^2} = -pr \frac{\partial^2 \varphi_2}{\partial t^2} \quad (31)$$

and after integration obtain

$$\frac{\partial \varphi_1}{\partial t} = \frac{pr}{q} \left(\Omega_2 - \frac{\partial \varphi_2}{\partial t} \right). \quad (32)$$

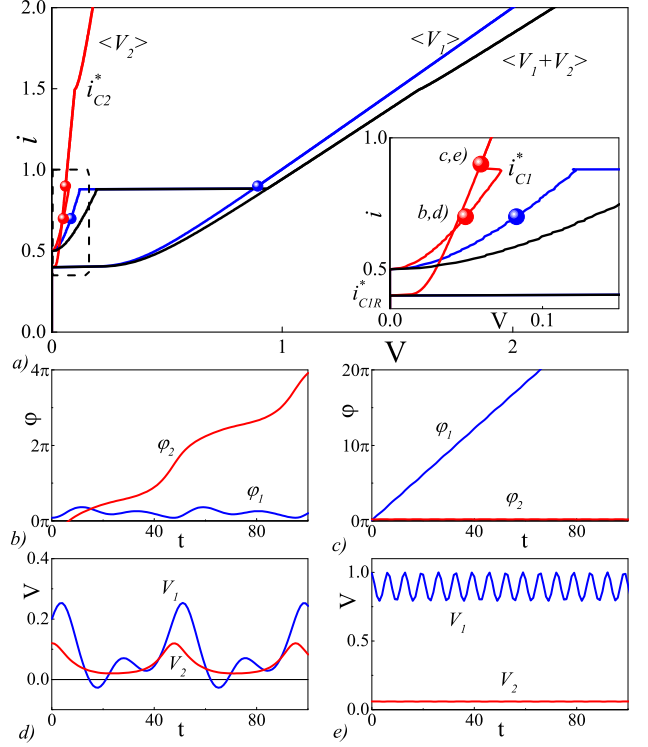


Figure 3: a) I-V characteristic of the asymmetric Josephson stack with coupling $\kappa = 0.2$. The black line demonstrates the IV dependence of the whole system, the blue line corresponds fast junction and red line describes slow junction. The panels b-e) show phase and voltage dynamics calculated b,c) at the current $i = 0.7$ below the switch of the fast junction into resistive state and d, e) at the current $i = 0.9$ over that switch. The other parameters are $r = 10$, $\beta = 10$, and $a = 0.5$.

The integration constant in (32) has been determined from the condition for the absence of intrinsic Josephson generation in fast junction. Substitution of (32) into (12) leads to the equation containing φ_2 only

$$i - \eta\Omega_2 = a \sin \varphi_2 + \frac{r}{(1 + \kappa r)} \frac{\partial \varphi_2}{\partial t}, \quad \eta = \frac{p^2 r^2}{q}. \quad (33)$$

Solution of this equation⁴⁷ has the form

$$\frac{d\varphi_2}{dt} = \frac{u(1 + \kappa r)}{r} \left[1 + 2 \sum_{n=1}^{\infty} \left(\frac{a}{i - \eta\Omega_2 + ua} \right)^n \cos \frac{ua(1 + \kappa r)}{r} nt \right], \quad (34)$$

where

$$u = \sqrt{(i - \eta\Omega_2)^2 / a^2 - 1} \quad (35)$$

is the average voltage across the slow junction. Carrying out in (34) averaging over the oscillation period for Ω_2 , we have

$$\Omega_2 = \frac{i^2 - a^2}{i\eta + a\sqrt{\eta^2 + r^2(i^2 - a^2)/(1 + \kappa r)^2}}. \quad (36)$$

Expressions (32), (35) and (36) determine the time evolution of a phase difference φ_1 on the fast junction

$$\varphi_1 = \varphi_{10} - \frac{2\kappa r}{(1+\kappa r)a} \sum_{n=1}^{\infty} \frac{1}{n} \left(\frac{a}{i - \eta\Omega_2 + ua} \right)^n \sin \frac{ua(1+\kappa r)}{r} nt \quad (37)$$

where φ_{10} is independent on time t phase difference across the fast junction. Averaging in (12) over period of slow junction frequency oscillations gives

$$i = \langle \sin \varphi_1 \rangle + pr\Omega_2. \quad (38)$$

From (37), (38) it follows that the critical current of the fast junction can be achieved at $i_{C1}^* < 1$. Indeed, even in the case when we restrict ourselves only to the first term of the series with respect to n we get that

$$i = \sin \varphi_{10} J_0 \left(\frac{2\kappa r}{(1+\kappa r)(i - \eta\Omega_2 + ua)} \right) + pr\Omega_2, \quad (39)$$

where $J_0(z) \leq 1$ is the zero order Bessel function.

The critical current i_{C1}^* is determined from (39) at $\sin \varphi_{10} = 1$ and it is affected by two physical mechanisms. The first one relates to the term $pr\Omega_2$ and correspond to appearance of the normal component of current through the fast junction similarly with Sec.III A. It tends to increase the i_{C1}^* up to $(1+\kappa)$. The second impact related with coefficient $J_0(z) \leq 1$ tends to decrease the critical current and it is explained by the presence of the oscillations of the phase φ_1 , which have significant amplitude unlike the previous subsection.

Figure 3 shows the results of numerical calculations follow from Eqs.(7)-(8) for the set of parameter relevant to the considered limit, namely, $\kappa = 0.2$, $r = 10$, $\beta = 10$ and $a = 0.5$. Black line in Fig. 3a is the IVC of the whole structure. Blue and red curves are IVC of the fast and the slow junctions, respectively. As shown in the Fig. 3a inset gives in more detail the initial part of IVC located in the dotted rectangle. The points on the curves mark the positions on the IVC at $i = 0.7$ and $i = 0.9$ for which the time dependences of the voltages $V_{1,2}$ and phase differences $\varphi_{1,2}$ across the contacts are shown in the Fig. 3b-Fig. 3e.

It can be seen from the Fig. 3a that as soon as the bias current i exceeds the critical current of slow junction a , a voltage drop occurs on both contacts. It increases with the i growth if $i \leq i_{C1}^* \approx 0.89$. Typical evolutions of $\varphi_{1,2}$ and $V_{1,2}$ at $i = 0.7$ is demonstrated at Fig. 3b and Fig. 3c, respectively. It is seen that in the considered bias current interval $a \leq i \leq i_{C1}^*$ there are the time oscillations of phase difference φ_2 across the slow junction superimposed on its linear growth, while the phase difference φ_1 oscillates with respect to a time-constant value. At $i = i_{C1}^* \approx 0.89$ there is a transition of the fast junction into resistive state, which, due to the large value of parameter β , is accompanied by a jump on the IVC to a region of high voltages. This circumstance substantially changes the balance of quasiparticle currents flowing into the s layer. If, at $i \leq i_{C1}^*$, the quasiparticles were injected into the s layer through slow contact, then at $i > i_{C1}^*$, a substantially large number of quasiparticles from the fast transition enters this layer and there is

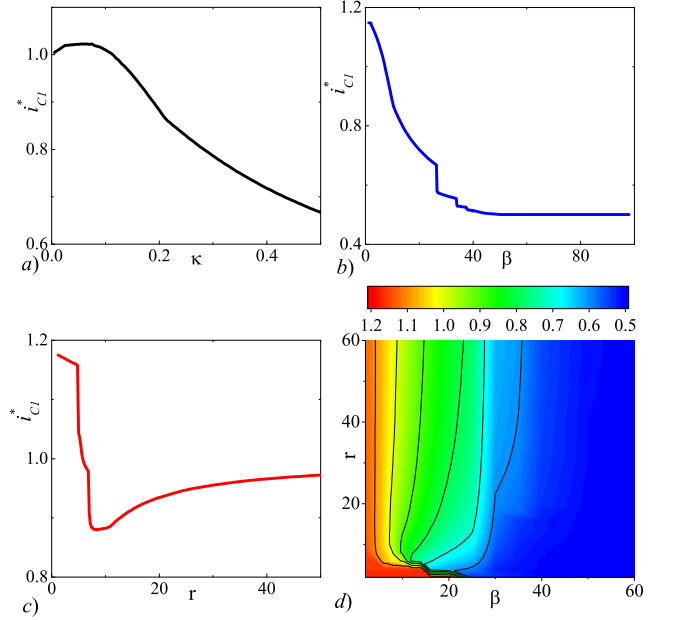


Figure 4: Dependence of the effective critical current i_{C1}^* of the fast junction versus a) coupling parameter κ , b) parameter β and c) ratio of resistances r . Panel d) demonstrates i_{C1}^* on the phase plain in coordinates β and r . The other parameters are $\kappa = 0.2$, $r = 10$, $\beta = 10$ and $a = 0.5$.

a change sign of potential Ψ . This results in increase of slow junction critical current to the value $i_{C2}^* = a(1+\kappa r)$, that is up to $i_{C2}^* = 3a$ for the chosen values of $\kappa = 0.2$ and $r = 10$. The slow junctions goes into superconducting state with independent in time φ_2 and V_2 (see Fig. 3d,e, which are provided the results of calculations for $i = 0.9 > i_{C1}^*$). From the Fig. 3c,e it is also easy to see that at $i = 0.9$ the phase difference φ_1 increases linearly with time, and the voltage drop V_1 oscillates around a constant value. At $i = i_{C2}^* = 3a = 1.5$ the slow junction contact switches to a resistive state, it is evident from the kink in its IVC. During the reverse motion along the I-V characteristic in the direction of decreasing the bias current i , the slow contact is first transitioned to the superconducting state at $i = i_{C2}^* = a(1+\kappa r)$, while the fast junction makes a similar transition abruptly at a current $i = i_{C1R}^* \approx 0.4 < a$.

Interestingly, for large β and κ , the effective critical current i_{C1}^* can become less than the critical current of the slow junction a . In this case transition of the slow junction into resistive state initiate the transition to the same state of the fast junction, the process takes place during the time $t \sim \Omega_2^{-1}$. The last transition switches the slow junction into the superconducting state and for $t \gtrsim \Omega_2^{-1}$ only fast junction is in the resistive state. Exactly this regime is predicted analytically by (39) in the case $\beta \rightarrow \infty$ for parameters $\kappa = 0.2$, $r = 10$ and $a = 0.5$. Fig.4 permits to check it, showing dependencies versus κ , β and r on the panels a), b) and c) respectively. While any of those parameters is small, that the critical current is larger than unity $i_{C1}^* > 1$ and tends to value $(1+\kappa)$. Increase of the parameters leads to the decrease of the i_{C1}^* , with significant drops on $i_{C1}^*(\beta)$ and $i_{C1}^*(r)$ dependencies. These drops

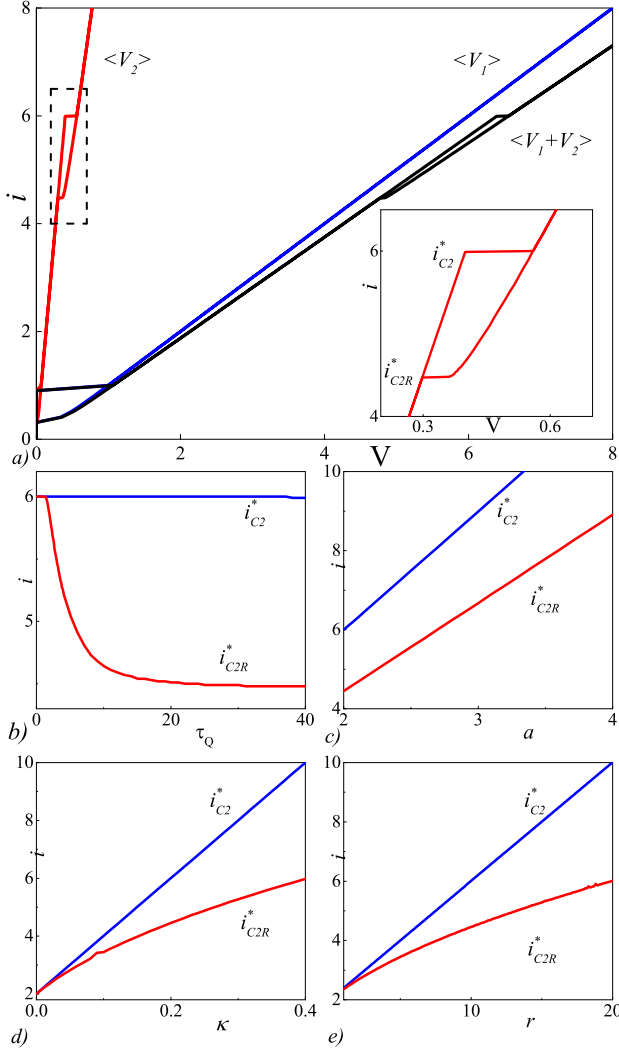


Figure 5: a) I-V characteristic of the asymmetric Josephson stack for slow relaxation $\tau_Q = 50$. The black line demonstrates the IV dependence of the whole system, the blue line corresponds fast junction and red line describes slow junction. Inset enlarges the area around critical current of the slow junction. b-e) Critical currents i_{C2}^* and i_{C2R}^* b) as function of relaxation time τ_Q , c) critical current a , d) coupling parameter κ and e) resistivity ratio r . The other parameters was taken from the set $\tau_Q = 50$, $r = 10$, $\kappa = 0.2$, $\beta = 10$ and $a = 2$.

are related with fulfillment of the condition $\beta\Omega_2 \gg 1$ and lead to the qualitative change of the phase dynamic. At very large $\beta > 50$ the critical current i_{C1}^* reaches the value $a = 0.5$ and becomes permanent. At Fig. 4d we show the i_{C1}^* dependence on the r - β plane and demonstrate that the latter regime appears at large β for a wide range of r .

IV. LARGE RELAXATION TIME $T_Q \gg 1$

In this approximation, the potential Ψ in the s layer does not have time to react to the instantaneous change in voltage at the

junctions and is determined by their time-averaged values

$$\Psi = \kappa(\langle V_1 \rangle - r\langle V_2 \rangle). \quad (40)$$

The correction to this solution of the equation (5) has the order of τ_Q^{-1} and is proportional to the difference of oscillating in time components $V_1 - \langle V_1 \rangle$ and $V_2 - \langle V_2 \rangle$ of voltage drops across the contacts. Substitution of (40) into (1), (3) gives

$$\frac{\partial \varphi_1}{\partial t} = V_1 + \kappa(\langle V_1 \rangle - r\langle V_2 \rangle), \quad (41)$$

$$\frac{\partial \varphi_2}{\partial t} = V_2 - \kappa(\langle V_1 \rangle - r\langle V_2 \rangle). \quad (42)$$

To demonstrate the specific features of the behavior of the structure under study in the limit of large τ_Q , it is enough to consider the case $a > 1$. At $1 < i < a$ the slow junction is in the superconducting state, while the fast one has switched to the quasiparticle branch of the I-V characteristic to the region of high voltages, where $i \approx \langle V_1 \rangle$ and

$$\varphi_1 = \Omega_1 t + \tilde{\varphi}_1. \quad (43)$$

The voltages V_1 and V_2 are almost permanent with a small periodic correction. In this way $V_{1,2} \approx \langle V_{1,2} \rangle$ and behaviour of the system is similar to that discussed in Subsec.III A. In particular, the critical current of the switching of the slow junction into resistive state, $i_{C2}^* = a(1 + \kappa r)$, is exactly the same as it was found in Subsec.III A.

However, after transition of the slow junction into the resistive regime this similarity is broken. In this case, at i slightly larger i_{C2}^* the slow junction generates periodic components $\tilde{\varphi}_{1,2}$,

$$\varphi_1 = \Omega_1 t + \tilde{\varphi}_1; \quad \varphi_2 = \Omega_2 t + \tilde{\varphi}_2, \quad (44)$$

which have an order of unity. This provides the significant difference between instantaneous values of $V_{1,2}$ and averaged $\langle V_{1,2} \rangle$ voltage. In this case, the averages are coupled similarly with (9)-(10) of Subsec III A.

$$\langle V_1 \rangle = q\Omega_1 + rp\Omega_2 \quad (45)$$

$$\langle V_2 \rangle = m\Omega_2 + p\Omega_1 \quad (46)$$

while the equations for periodic component are similar with equations for separate junctions with modified effective bias currents

$$i + p(\Omega_1 - r\Omega_2) = \sin(\varphi_1) + \frac{\partial \varphi_1}{\partial t} + \beta \frac{\partial^2 \varphi_1}{\partial t^2} \quad (47)$$

$$i - rp(\Omega_1 - r\Omega_2) = a \sin(\varphi_2) + r \frac{\partial \varphi_2}{\partial t} \quad (48)$$

Since the fast junction stays on the resistive branch of IVC, we can neglect averaged part of $\sin(\varphi_1)$ term in Eq. 47 and get the equality

$$i = q\Omega_1 + pr\Omega_2, \quad (49)$$

which transforms the Eq. (48) into

$$\frac{i + \kappa r^2 \Omega_2}{(1 + \kappa r)} = a \sin(\varphi_2) + r \frac{\partial \varphi_2}{\partial t} \quad (50)$$

having solution⁴⁷

$$\frac{d\varphi_2}{dt} = \frac{u}{r} \left[1 + 2 \sum_{k>0} \left(\frac{a}{i_{eff2} + ua} \right)^k \cos \frac{ua(1 + \kappa r)}{r} kt \right], \quad (51)$$

$$u = \sqrt{i_{eff2}^2/a^2 - 1}; \quad i_{eff2} = \frac{i + \kappa r^2 \Omega_2}{(1 + \kappa r)}. \quad (52)$$

After time averaging in (51) we get the equation for Ω_2

$$\Omega_2 = \frac{u}{r} = \frac{1}{r} \sqrt{\left(\frac{i + \kappa r^2 \Omega_2}{a(1 + \kappa r)} \right)^2 - 1}, \quad (53)$$

which has the solution

$$\Omega_2 = \frac{i\kappa r + i_{C2}^* \sqrt{i^2 + \kappa^2 r^2 - i_{C2}^{*2}}}{r(i_{C2}^{*2} - \kappa^2 r^2)} \quad (54)$$

The slow junction stays in the resistive state until the expression under the root crosses zero. Then, the slow junction returns into the superconducting state at bias current $i = i_{C2R}^*$,

$$i_{C2R}^* = \sqrt{i_{C2}^{*2} - \kappa^2 r^2}. \quad (55)$$

Numerical solution of the (1)-(5) for finite values of parameters qualitatively confirms the analytical estimates. The I-V curve of the considered system for the large relaxation time $t_Q = 50$ is demonstrated in the Fig. 5a (the other parameters are the same with Fig. 2: $a = 2$, $r = 10$, $\kappa = 0.2$, $\beta = 10$). Inset of Fig. 5a enlarges the vicinity of the critical point for the slow junction V_2 . It is clear, that its transition to the resistive state occurs abruptly when the bias current reaches the value $i_{C2}^* = a(1 + \kappa r) = 6$. However, during the decrease of the bias current, the slow junction stays in the resistive state until the current $i_{C2R}^* \approx 4.4$. In Fig. 5b we demonstrate the evolution of the critical i_{C2}^* and return current i_{C2R}^* as a function of t_Q . The return current starts to decrease when the t_Q is comparable with $\omega_{C1}^{-1} = 1$, and reaches the asymptote when t_Q significantly exceeds the $\omega_{C2}^{-1} = r = 10$. The dependencies of the i_{C2}^* and i_{C2R}^* on parameters a , κ and r are shown in the Fig.5c-e. The i_{C2R}^* curves have the shape close to that followed from (55) with linear dependence versus a , and root-like versus κ and r . The exact values of the return current is smaller than analytical estimates, due to limited validity of approximation (49) at the finite β , and, thus, the hysteresis loop becomes more noticeable.

V. DISCUSSION

In the paper we consider analytically and numerically the dynamics of the asymmetric Josephson stack with two inequivalent junctions: the fast capacitive junction JJ_1 and slow non-capacitive junction JJ_2 . The quasiparticle imbalance in the thin superconducting layer between junctions leads to significant changes of the system dynamical properties:

1) If the fast junction is in the resistive state, and slow junction is in the superconducting state, then the effective critical current i_{C2}^* of the slow junction is growing up. This effect is stronger for junctions with higher ratio of resistances.

2) In the case of slow junction in resistive state and fast junction in superconducting state, the effective critical current i_{C1}^* of the fast junction may be either increased or decreased depending on parameters of the system. Numerical solution demonstrates that its effective critical current is increased for the weak coupling κ , small resistance ratio r and small parameter β , while at the large parameters it is decreased.

3) If the quasiparticle relaxation is slower than Josephson times $t_Q \gg \omega_{C1,2}^{-1}$, the coupling is leading to hysteresis on the current-voltage characteristic of slow non-capacitive junction. The quasiparticle injection through the slow junction leads to increase of its generation frequency Ω_2 and provides some kind of resistive branch of IVC for non-capacitive junction.

Features on the IVC at subgap voltages similar to those obtained in this study were previously observed in double-barrier SI_1sI_2S structures⁴⁸⁻⁵⁰. However, they were not the subject of study in these structures. It is for this reason; a quantitative comparison of the predictions of the developed model with these experimental data is difficult. For instance, it is unclear how to distinguish the modified critical currents of the junctions $i_{C1,2}^*$ from their truly critical currents $i_{C1,2}$. However, it may be possible if one of the junctions has widely variable parameters, for instance, as in Josephson spin-valve devices. One can smoothly modify their critical current with remagnetization of the ferromagnetic layer, providing the transition between the regimes of Sec.III A and III B. It gives a possibility to measure as well as the truly critical current as the modified one for the both junctions.

Even more intriguing case occurs for the junction with controllable $0-\pi$ transition^{51,52}, at which the critical current of the junction changes on the orders of magnitude. Moreover, the hysteretic nature of considered effect can lead to the different dynamical states inside $0-\pi$ transition performed with or without bias current.

Acknowledgments. The authors acknowledge helpful discussions with Yu. M. Shukrinov, V. V. Bol'ginov and D. A. Ryndyk. The analytical study was supported by RFBR (18-32-00672 mol-a) and numerical calculations were done with support of Russian Science Foundation (17-12-01079).

¹ Eschrig M 2015, Reports on Progress in Physics, **78**, 104501.

² Linder J, Robinson J W A 2015, Nature Physics, **11**, 307.

- 3 Blamire M G, Robinson J W A 2014, *Journ. Phys. Cond. Mat.*, **26**, 453201.
- 4 Soloviev I I, Klenov N V, Bakurskiy S V, Yu M Kupriyanov, Gudkov A L, and Sidorenko A S 2017, *Beilstein Journal of Nanotechnology*, **8**, 2689.
- 5 Baek B, Rippard W H, Benz S P, Russek S E, and Dresselhaus P D 2014, *Nature Communications*, **5**, 3888.
- 6 Gingrich E, Niedzielski B M, Glick J A, Wang Y, Miller D, Loloee R, Pratt W Jr, and Birge N O 2016, *Nature Physics* **12**, 564.
- 7 Alidoust M, Halterman K 2014, *Phys. Rev. B* **89**, 195111.
- 8 Iovan A, Golod T, and Krasnov V M 2014 *Phys. Rev. B* **90**, 134514.
- 9 Ouassou J A, Linder J 2017, *Phys. Rev. B* **96**, 064516.
- 10 Klenov N V, Khaydukov Yu N, Bakurskiy S V, Morari R, Soloviev I I, Boian V, Keller T, Kupriyanov M Yu, Sidorenko A S and Keimer B 2018, arXiv:1809.10165.
- 11 Larkin T I, Bolginov V V, Stolyarov V S, Ryazanov V V, Vernik I V, Tolpygo S K, and Mukhanov O A 2012, *Appl. Phys. Lett.* **100**, 222601.
- 12 Bakurskiy S V, Klenov N V, Soloviev I I, Kupriyanov M Yu, and Golubov A A 2013, *Phys. Rev. B* **88**, 144519.
- 13 Ruppelt N, Sickinger H, Menditto R, Goldobin E, Koelle D, Kleiner R, Vavra O, Kohlstedt H 2015, *Appl. Phys. Lett.*, **106**, 022602.
- 14 Vernik I V, Bol'ginov V V, Bakurskiy S V, Golubov A A, Kupriyanov M Yu, Ryazanov V V and Mukhanov O A 2013, *IEEE Tran. Appl. Supercond.*, **23**, 1701208.
- 15 Bakurskiy S V, Klenov N V, Soloviev I I, Bol'ginov V V, Ryazanov V V, Vernik I I, Mukhanov O A, Kupriyanov M Yu, and Golubov A A 2013, *Appl. Phys. Lett.* **102**, 192603.
- 16 Bakurskiy S V, Klenov N V, Soloviev I I, Yu M Kupriyanov, and Golubov A A 2016, *Appl. Phys. Lett.*, **108**, 042602.
- 17 Bakurskiy S V, Filippov V I, Ruzhickiy V I, Klenov N V, Soloviev I I, Yu M Kupriyanov, and Golubov A A 2017, *Phys. Rev. B* **95**, 094522.
- 18 Bakurskiy S V, Klenov N V, Soloviev I I, Pugach N G, Kupriyanov M Yu, and Golubov A A 2018 *Appl. Phys. Lett.* **113**, 082602.
- 19 Zhu Y, Pal A, Blamire M G, Barber Z H 2017, *Nature Materials*, **16**, 195.
- 20 De Simoni G, Strambini E, Moodera J S, Bergeret S, Giazotto F 2018, *Nano Lett.*, **18**, 6369.
- 21 Pugach N G, Kupriyanov M Yu, Goldobin E, Kleiner R, and Koelle D 2011 *Phys. Rev. B* **84**, 144513.
- 22 Li C, de Boer J C, de Ronde B, Ramankutty S V, van E Heumen, Huang Y, de Visser A, Golubov A A, Golden M S, Brinkman A 2018, *Nature Materials*, **17**, 875.
- 23 Belzig W, Wilhelm F K, Bruder C, Schon G, Zaikin A D 1999, *Superlattices and microstructures*, **25**(5-6), 1251.
- 24 Brinkman A, Golubov A A, Rogalla H, Wilhelm F K, and Kupriyanov M Y 2003, *Phys. Rev. B*, **68**, 224513.
- 25 Nevirkovets I P, Evetts J E, and Blamire M G 1994, *Physics Letters A* **187**, **1**, 119.
- 26 Shafranjuk S E, Tachiki M, and Yamashita T 1996 *Phys. Rev. B* **53**, 15136.
- 27 Sakai S, Bodin P, and Pedersen N F, *Appl. J* 1993 *Phys.*, **73**, 2411.
- 28 Ustinov A V, Kohlstedt H, Cirillo M, Pedersen N F, Hallmanns G, and Heiden C 1993 *Phys. Rev. B* **48**, 10614(R).
- 29 Kleiner R and Muller P 1994, *Phys. Rev. B* **49**, 1327.
- 30 Kleiner R, Muller P, Kohlstedt H, Pedersen N F, and Sakai S 1994 *Phys. Rev. B* **50**, 3942.
- 31 Bulaevskii L N, Dominguez D, Maley M, Bishop A, and Ivlev B 1996, *Phys. Rev. B* **53**, 14 601.
- 32 Hu X, Lin S Z 2010, *Superconductor Science and Technology*, **23**(5), 053001.
- 33 Koyama T, Tachiki M 1996, *Phys. Rev. B*, **54**, 16183.
- 34 Matsumoto H, Sakamoto S, Wajima F, Koyama T, Mashida M 1999, *Phys. Rev. B*, **60**, 3666.
- 35 Machida M, Koyama T, and Tachiki M 1999 *Phys. Rev. Lett.* **83**, 4618.
- 36 Shukrinov Yu M, Mahfouzi F 2006, *Physica C: Superconductivity and its applications*, **434**(1), 6.
- 37 Shukrinov Yu M, Mahfouzi F 2007, *Phys. Rev. Lett.* **98**, 157001.
- 38 Shukrinov Yu M, Rahmonov I R 2012, *JETP Lett.* **115**(2), 289.
- 39 Ryndyk D A 1997, *JETP Lett.*, **65**(10), 791.
- 40 Artemenko S and Kobelkov A 1997, *Phys. Rev. Lett.* **78**, 3551.
- 41 Ryndyk D A 1998, *Phys. Rev. Lett.* **80**, 3376.
- 42 Shafranjuk S E and Tachiki M 1999, *Phys. Rev. B* **59**, 14087.
- 43 Ryndyk D A, *Eksp. Zh* 1999 *Teor. Fiz.* **116**, 1798 (1999); [*JETP* **89**, 975].
- 44 Rother S, Koval Y, Muller P, Kleiner R, Ryndyk D A, Keller J, and Helm C 2003, *Phys. Rev. B* **67**, 024510.
- 45 Keller J, and Ryndyk D A 2005, *Phys. Rev. B* **71**, 054507.
- 46 Volkov A F 2007 *Phys. Rev. B*, **76**, 174502.
- 47 Aslamazov L G, Larkin A I, Ovchinnikov Yu N 1968, *Sov. Phys. JETP* **28**, 171.
- 48 Balashov D, Buchholz F I, Schulze H, Khabipov M I, Dolata R, Kupriyanov M Y, and Niemeyer J 2000, *Superconductor Science and Technology*, **13**, 244.
- 49 Tolpygo S K, Brinkman A, Golubov A A, and Kupriyanov M Yu 2003, *IEEE Tran. Appl. Supercond.*, **13**, 138.
- 50 Nevirkovets I P, Shafranjuk S E, and Ketterson J B 2003, *Phys. Rev. B* **68**, 024514.
- 51 Ryazanov V V, Oboznov V A, Rusanov A Yu, Veretennikov A V, Golubov A A, and Aarts J 2001, *Phys. Rev. Lett.* **86**, 2427.
- 52 Oboznov V A, Bol'ginov V V, Feofanov A K, Ryazanov V V and Buzdin A I 2006, *Phys. Rev. Lett.* **96**, 197003.